INFLUENCE OF SIDE-IMPACTING DYNAMIC ARMOUR COMPONENTS ON LONG ROD PROJECTILES

Ewa Lidén, Olof Andersson, Anders Tjernberg

FOI, Swedish Defence Research Agency, Defence & Security Systems and Technology Division, Grindsjön, SE-14725 Tumba, Sweden

Using add-on armour components to disturb long rod projectiles (LRP) before they hit the basic armour is a weight efficient way of increasing the protection of lighter vehicles. In this study, the effect of moving armour components, in the form of one or three cylindrical rods, hitting the side of the LRP, was investigated. The rods were hitting the side of the LRP at an angle of attack of 60 degrees. Rod velocities of 200 and 600 m/s and hitting points in the front and in the middle of the LRP were studied. The velocity of the LRP was 2000 m/s. The study is based on small scale reverse impact experiments and continuum dynamic simulations.

To break the LRP, high rod velocities must be used. One rod hitting the LRP at 200 m/s gives approximately the same effect (some yaw but no fracture) as that of a moving oblique plate having the same velocity and angle of obliquity. Increasing the velocity of the rod to 600 m/s resulted in fracture of the LRP closely behind the hitting point both when hitting the front and the middle of the LRP. When using three rods, fracture was only obtained when the hitting points of the rods were closely spaced.

INTRODUCTION

Armour against long rod projectiles (LRP) often include dynamic components that disturb, deform or fragment the projectile. Examples of such armours are reactive armour or sensor-activated armour. In a reactive armour the protective components are moving plates activated by the projectile. In a sensor-activated armour, the design of the hard kill component can vary and the interaction usually occurs at a greater distance from the vehicle than is the case with a reactive armour.

The effect of penetrating moving thin plates has been studied earlier [1, 2]. In this study, the effect of moving armour components hitting the side of the projectile was investigated. This question has also been addressed before. In [3] the effect of a steel sphere hitting the side of the projectile was investigated. In this study the armour component is a cylindrical rod. The effect of hitting point, rod velocity and the number of rods is investigated.

EXPERIMENTS

Tungsten long rod projectiles, $L/D = 30$, were impacted at the side of the projectiles by one or three steel rods with the same diameter D as the projectile. The reverse impact experiments were carried out using a two-stage light-gas gun. The projectile was a diameter 2 mm, length 60 mm straight cylinder (no threads, nose or fins), made of a sintered tungsten alloy (Y925 from Kennametal Hertel AG [4]). The projectile velocity was 2000 m/s. The rods were 2 mm diameter cylinders made of steel (SS 2541-03) impacting perpendicular to the projectile at 60º angle, see Figure 1. The hitting point along the projectile, when using one rod, was one projectile diameter from the front of the projectile and at the middle of the projectile respectively. The velocity of the rod was 200 and 600 m/s respectively.

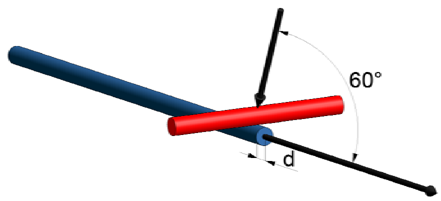

Figure 1. The armour component consisting of a rod perpendicular to the projectile impacting the side of the projectile at 60º angle.

When using three rods, the hitting points were distributed along the projectile. In the 600 m/s rod velocity case, two different hitting point patterns were studied: one where the rods had the same distance between each other as in the 200 m/s case, and one where the hitting points on the projectile agreed with the 200 m/s case, see figure 2. The cases studied are summarized in Table 1.

The geometry and position of the projectile after the interaction with the rods and the velocities achieved were evaluated from flash X-ray pictures. The projectile was registered with a pre-launch exposure (as a reference) and at two or three times after initial contact between the (first) rod and the projectile. These pictures were adjusted for the non-coinciding positions of the X-ray flashes resulting in figures showing only the deformation and the translation caused by the interaction. The surface of the projectiles was inspected after the interaction to establish the duration of the interaction between the rods and the projectile.

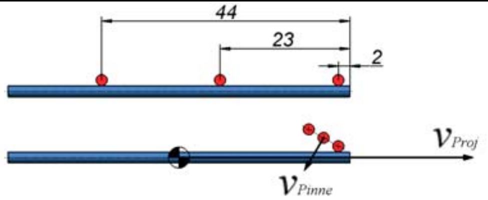

Case 5. Rod velocity 200 m/s.

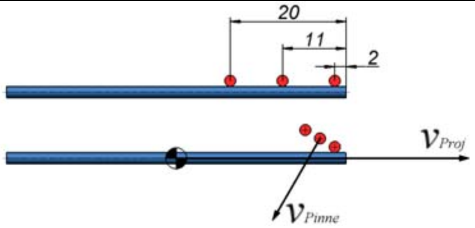

Case 6. Rod velocity 600 m/s. Same rod distances as in the 200 m/s case.

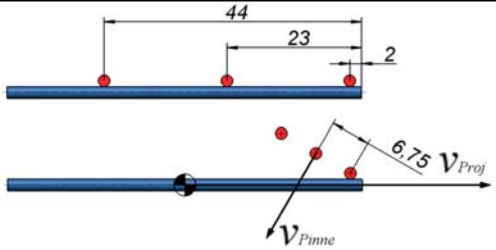

Case 7. Rod velocity 600 m/s. Same hitting points as in the 200 m/s case.

Figure 2. Hitting points along the projectile as a result of the relation between the rod distances, the rod velocity and the projectile velocity.

Table 1. Cases studied.

Case	Hitting point	Velocity [m/s]	Number of rods	Distances between the rods [mm]	Distances between the hitting points on the projectile [mm]
1	In the front	200	1	-	-
2	In the front	600	1	-	-
3	Middle	200	1	-	-
4	Middle	600	1	-	-
5	Distributed along whole of the projectile	200	3	3	21
6	Distributed along part of the projectile	600	3	3	9
7	Distributed along whole of the projectile	600	3	6.75	21

SIMULATIONS

AUTODYN-3D (v 6.1) was used for the numerical simulations with Lagrange formulation and the (instantaneous) erosion strain set to 1.5. For both the projectile and the rods, the Johnson-Cook (J-C) strength model was used. The strength parameters used were based on material investigations and estimations according to [4, 5], see Table 2. The reference strain rate $\dot{\varepsilon}_0$ is set to 1.0 s^{-1}.

Table 2. Parameters used in the J-C strength model for the rod and the projectile materials.

Parameter	Steel SS2541-03	Tungsten alloy Y925
A	750 MPa	631 MPa
B	1150 MPa	1258 MPa
n	0.49	0.092
C	0.014	0.014
m	1.0	0.94
T_{melt}	1700º K	1720º K
$\dot{\varepsilon}_0$	1.0 s^{-1}	1.0 s^{-1}

For steel, a linear equation of state (EOS) was used with a bulk modulus of 172 GPa and a shear modulus of 79 GPa. For the tungsten material, EOS-parameters from the AUTODYN material library were used [6].

For the projectile, the J-C fracture model was used with parameters as shown in Table 3. No failure criterion (only numerical erosion) was used for the rods.

Table 3. Parameters in the J-C fracture model for the projectile.

Parameter	Tungsten alloy Y925
D_2	0.27
D_3	-3.4
D_1; D_4; D_5	0

RESULTS

Figure 3 shows the registrations and the evaluated pictures (adjustment for the non-coinciding positions of the X-ray flashes) from the experiments. The pictures show that the higher velocity is required to achieve fracture of the projectile, and that if more than one rod is used the hitting points should be narrow spaced.

Figure 4 shows photos of the projectiles after the interaction with the rod. The contact surfaces resulting from the interaction are identified and their position and length are evaluated. In the cases where the projectile is broken, the position of the fracture is also evaluated. Table 4 summarizes the evaluation. Unfortunately the projectile from case 1 could not be retrieved and thus could not be evaluated with respect to the contact surface. Some of the projectiles are bent and in one case fractured (case 5) after the interaction event, probably when hitting the wall of the tank system where the experiments were performed.

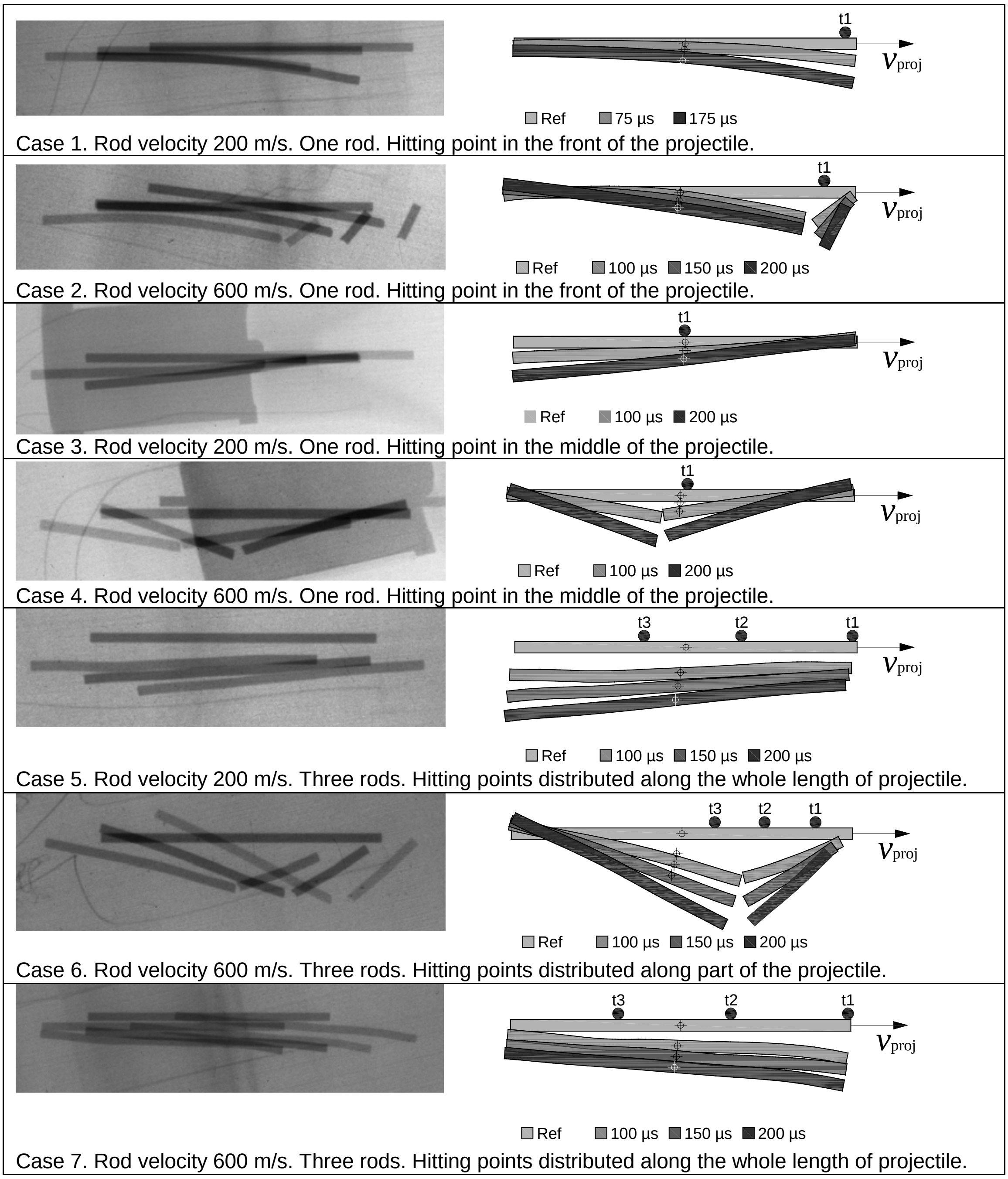

Figure 3. Results from experiments. To the left: the X-ray registrations, to the right: the evaluated pictures showing the deformation and translation caused by the interaction.

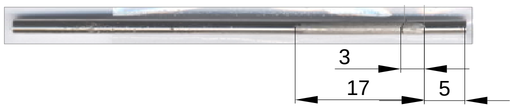

Case 2. Rod velocity 600 m/s. One rod. Hitting point in the front of the projectile.

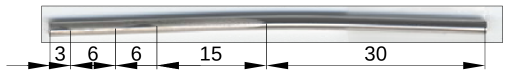

Case 3. Rod velocity 200 m/s. One rod. Hitting point in the middle of the projectile.

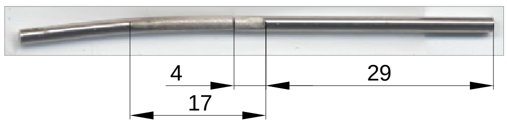

Case 4. Rod velocity 600 m/s. One rod. Hitting point in the middle of the projectile.

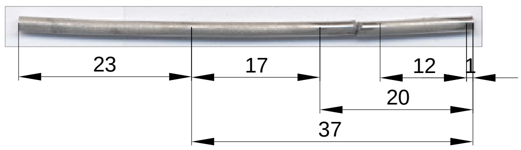

Case 5. Rod velocity 200 m/s. Three rods. Hitting points distributed along the projectile.

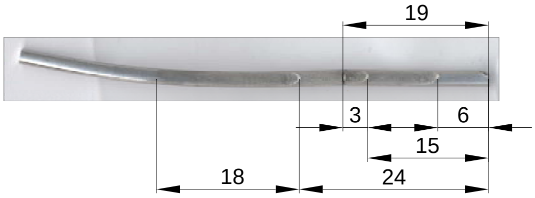

Case 6. Rod velocity 600 m/s. Three rods. Hitting points distributed along part of the projectile.

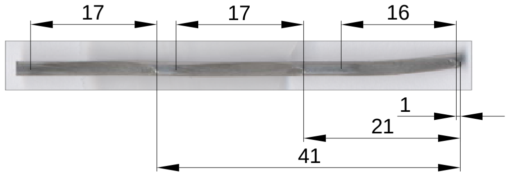

Case 7. Rod velocity 600 m/s. Three rods. Hitting points distributed along of the projectile.

Figure 4. Contact surfaces on the projectile resulting from the interaction with the rods. The measurements indicate the position and length of the interaction and the position of fracture in the cases where the projectile was broken.

Table 4. The position and length of the contact surface between the rod and the projectile and the position of fracture of the projectile.

Case	Distance between contact surface and front of projectile [mm]		Length of contact surface [mm]	Distance between fracture and front of projectile [mm]	Distance between fracture and hitting point [mm]
	Desired	Achieved			
1	2	-	-	No fracture	No fracture
2	2	5	17	8	3
3	30	30	15 (30)	No fracture	No fracture
4	30	29	17	33	4
5	2 23 44	1 20 37	11 17 23	No fracture	No fracture
6	2 11 20	6 15 24	- - 18	- 19 -	- 3 -
7	2 23 44	1 21 41	14 17 17	No fracture	No fracture

Figure 5 shows results from the simulation of case 2, one rod impacting the projectile at 600 m/s in the front of the projectile. The left picture indicates that the rod slides along the projectile, heavily deforming, and that the nose of the projectile will be broken. The right picture indicates a position of the fracture coinciding with the position achieved in the experiment (2.6 mm from the hitting point to be compared with 3 mm in the experiment). In the case of 200 m/s the simulation indicated that no fracture of the projectile took place.

Figure 5. Simulation of one rod hitting the projectile at 600 m/s in the front of the projectile (case 2). To the left: material properties at 4.5 μs after hit. To the right: the frontal part of the projectile indicating the position of fracture.

Figure 6 shows results from the simulation of case 7, three rods impacting the projectile at 600 m/s distributed along the whole length of the projectile. In this case, the simulation indicates fractures from all the rod impacts although the experiment did not result in any fracture at all.

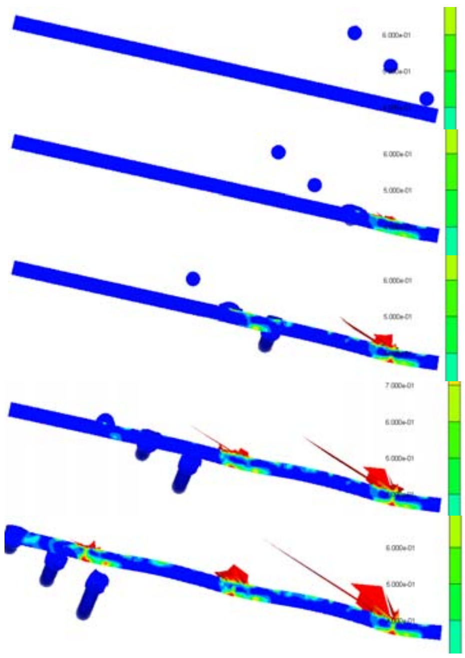

Figure 6. Simulation of three rods hitting the projectile at 600 m/s distributed along the whole length of the projectile (case 7).

DISCUSSION

The interaction resulted in the cases of 200 m/s rod velocity in a rotation of the projectile, giving approximately the same amount of yaw irrespective of the hitting point and the number of rods.

At a rod velocity of 600 m/s, the projectile fractured except for the case with three rods distributed over the whole length of the projectile (case 7). The behaviour of the fractured rods was roughly the same for the case of one rod (case 2 and 4) and three closely spaced rods (case 6). In the case of fracture, the fracture surface is roughly perpendicular to the axis of the projectile and situated at a distance of 1.5 - 2 projectile diameters behind the (initial) hitting point.

The numerical simulations showed good agreement with the experiments when the effect of one rod was investigated, but overestimated the risk of fracture for three rods. According to the simulation of case 7, the rods seem to interact with the projectile independent of each other. This results in three fractures in the simulation, whereas the experiments only show one (case 6) or no (case 7) fracture.

CONCLUSIONS

Rods hitting the side of an LRP can constitute weight-efficient hard-kill components in a sensor-activated armour. A steel rod having the same diameter as the LRP hitting the LRP at 200 m/s gives approximately the same effect (some yaw but no fracture) as that of a steel plate having the same thickness (one projectile diameter), velocity and angle of obliquity. Using three rods at this velocity did not change the behaviour of the residual projectile.

Increasing the velocity of the rod to 600 m/s resulted in fracture of the LRP. When using three rods, fracture was only obtained when the hitting points on the LRP were closely spaced. Thus, the terminal ballistic value of hitting the LRP with more than one rod is doubtful.

REFERENCES

[1] E. Lidén, B. Johansson, B. Lundberg, Effect of thin oblique moving plates on long rod projectiles: A reverse impact study, *Int. J. Impact Engng.,* **32**, 1696-1720 (2006)
[2] E. Lidén, O. Andersson, B. Lundberg, Influence of plate and projectile partameters on the interaction between long rod projectiles and thin oblique plates, *Int. J. Impact Engng.,* Submitted for publication (2006)
[3] S. Mousavi, E. Lidén, Interaction of long rod projectiles with side impacting fragments. *18th International Symposium on Ballistics*, Vol 2 1049-1056 (1999).
[4] P. Skoglund, Constitutive modelling of a tungsten heavy metal alloy, *J. Phys.* IV, 207-212 France 110 (2003)
[5] E. Lidén, J. Ottosson, L. Holmberg, WHA long rods penetrating stationary and moving oblique steel plates. *16th International Symposium on Ballistics*, Vol 3, pp 703-712 (1996).
[6] Group GMX-6(1969), Selected Hugoniots, *Los Alamos Scientific Laboratory Report LA- 4167-MS.*